School of Pharmacy[1], Curtin University; Curtin Health and Innovation Research Institute of Aging and Chronic Disease[2], Curtin University, Bentley, Australia

# Stimulation of bone regeneration with pigment epithelium-derived factor microparticles: evidence *in silico*, *in vitro* and *in vivo*

P. X. Lee[1], J. Martinez[1], C. R. Dass[1,2]

*Received January 16, 2016, accepted April 10, 2016*

*Professor Crispin R. Dass, School of Pharmacy, Curtin University, GPO Box U1987, Perth 6845, Australia*
*crispin.dass@curtin.edu.au*

*Pharmazie 71: 382–389 (2016)* *doi: 10.1691/ph.2016.6010*

The occurrence of bone defects can be due to a variety of factors not limited to bone fractures and tumours. Most diseased bone is removed and the patient fitted with prosthetics, prior to use of certain factors such as bone morphogenetic proteins (BMPs) to aid healing. Recently, the protein pigment epithelium-derived factor (PEDF) and the polysaccharide chitosan have been found to have promising effects on the regeneration of bone, with the major advantage of these agents being their safety to date. A study was performed to determine whether the combination of both chitosan and PEDF would enhance greater bone regeneration effects. Post-formulation, *in silico* tests (particle sizing and surface charge determination) were followed by several cell-based assays (microparticle cellular uptake, cytotoxicity, mitochondrial abundance, bone mineral formation, colony formation in matrigel, and colony formation in collagen I matrix), and finally *in vivo* testing where microparticles were injected periosteally in the hindlimb. Collectively, these findings support the idea that PEDF microencapsulated within chitosan promotes bone regeneration, and has potential for bone trauma management. Future studies will examine the ability of this promising bone regeneration microparticle to heal bone in disease states such as fracture and tumour-mediated osteolysis.

## 1. Introduction

Bone is a tissue capable of intrinsic regenerative properties (Papadimitropoulos et al. 2015). This is based on the healing processes which lead to the formation and restoration of bone tissue functionality (Lin et al. 2015). However, there are limitations to its potential to regenerate when it comes to critical bone defects (Shrivats et al. 2014). Lesions of the bone beyond a critical size can lead to scarring rather than being regenerated, resulting in non-union (Petite et al. 2000). Therefore, therapeutic aids to bone regeneration are required.

At present, autologous or allogeneic bone grafts are routinely used to treat critical bone defects attributed to infections, tumours and traumas (Papadimitropoulos et al. 2015). However, shortcomings of utilising these which include high risk of infections, hinder their use for bone repair. Therefore, in the present study, we examined the feasibility of two biologicals [(pigment epithelium-derived factor (PEDF) protein encapsulated within a chitosan polysaccharide microparticle)] for bone regeneration capacity.

PEDF is a natural 50kDa glycoprotein found endogenously in the human body, responsible for the inhibition of angiogenesis (Broadhead et al. 2009, 2010). It is secreted by mesenchymal stem cells (MSCs) undergoing osteogenic differentiation (Li et al. 2012). PEDF has been demonstrated to be a promising biological drug candidate with low toxicity and high stability (Ek et al. 2007a), but its delivery requires a suitable drug delivery system. An ideal delivery vehicle with features such as being biocompatible, non-toxic, non-immunogenic, biodegradable, inexpensive to formulate, able to release the carried agent in a controlled manner, able to carry a variety of molecular agents without changing its own chemical constitution and not require unsafe formulation procedures for manufacture is needed. One of the most suitable materials that hold these properties is chitosan (Cheng et al. 2009; Tan et al. 2009).

Chitosan is a naturally-derived polysaccharide that is cationic in nature, enabling the formulation of stable ionic complexes with water-soluble anionic molecules under physiological conditions (Tan et al. 2009). It is derived predominantly from the shells of crustaceans, and thus has an abundant supply. It has been used to deliver growth factors such as platelet-derived growth factor (PDGF) and tumour growth factor β (TGF-β) to MSCs for more effective repair of fractures (Tan et al. 2014). Due to its biocompatibility, non-toxicity, antibacterial ability and biodegradability, chitosan is widely utilised for the regeneration of bone tissues (Dash et al. 2011). Furthermore, despite its low mechanical strength, it possesses excellent biological properties, high hydrophilicity, low cost and has properties conducive to the organic nature of bone tissue (Serra et al. 2015; Jiang et al. 2014).

In this study, results from a variety of *in silico*, *in vitro* and *in vivo* studies are described. We tested whether PEDF encapsulated within chitosan microparticles can promote bone regeneration *in vivo*. MSCs were used in most of the *in vitro* studies as precursor cells as they possess the potential to differentiate and proliferate into osteoblasts (cells that form bone matrix) (Vimalraj and Selvamurugun 2014). Furthermore, we looked at mitochondrial health, viability, colony formation and bone mineral formation in these cells. As a result, the series of studies have shown that CMPs encapsulating PEDF have potential for bone regeneration.

## 2. Investigations and results

### 2.1. Formulation and analysis

In order to enhance the effects of bone regeneration, we encapsulated PEDF into chitosan microparticles (CMPs) using a vortex-assisted complex coacervation method. Both types of particles (CMPs and EMPs) assumed an initial opalescent suspension that slowly sedimented upon storage at room temperature (~ 20 °C) for 24 h (**Fig. 1A**). Sedimentation seemed to occur faster with the CMP formulation, perhaps due to the extra charge conferred upon the formulation due to PEDF, which has charged regions. Particles formed a pellet upon centrifugation leaving a clear supernatant (indicating that all particles were deposited) (**Fig. 1B**), but pellets were easily resuspended upon

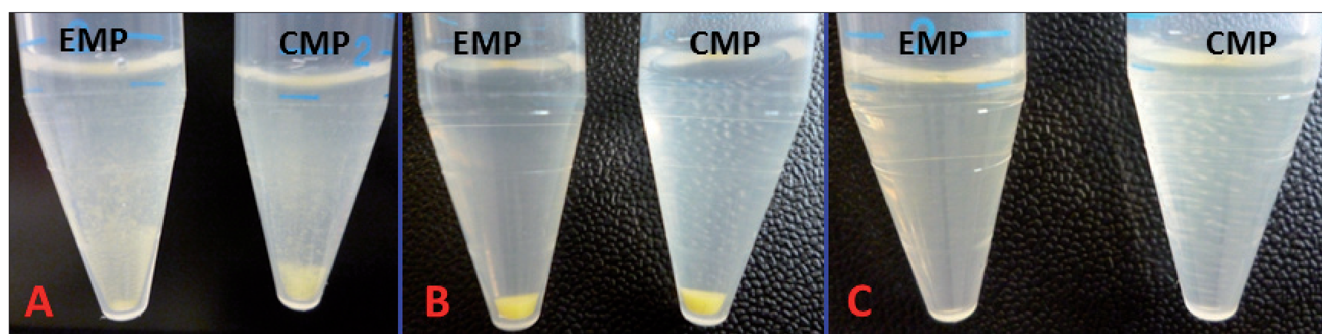


Fig. 1: Appearance of microparticles. (**A**) The appearance of microparticles with and without pigment epithelium-derived factor (PEDF) 24 hours post-manufacture, stored at room temperature, ~20 °C. (**B**) Microparticle suspensions centrifuged at 1000*g* for 1 minute. (**C**) Supernatants that contained the unbound PEDF were removed and the microfuge tube resuspended.

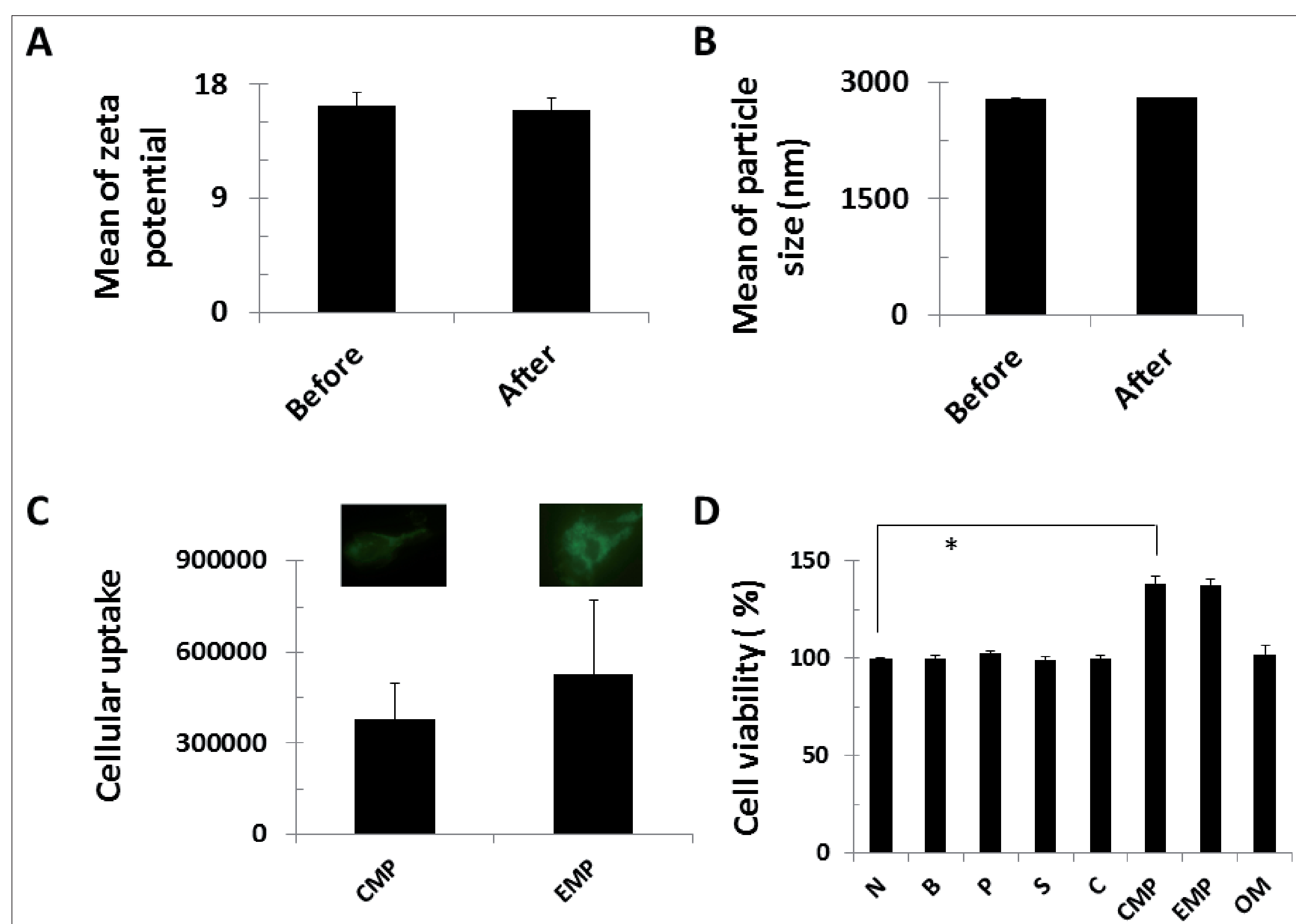


Fig. 2: Microparticle biophysical characterisation and effect on viability of mesenchymal stem cells (MSCs). (**A**) Mean zeta potential of CMP tested on the day of formulation (before) and 3 months post-formulation (after). (**B**) Mean particle size of CMP tested on the day of formulation (before) and 3 months post-formulation (after). (**C**) Uptake of FITC-labelled CMP and EMP into MSCs. (**D**) Viability of (MSCs) in the presence of the non-treated (N), BSA (B), pigment epithelium-derived factor, PEDF (P), starch (S), free chitosan (C), PEDF encapsulated within chitosan microparticles (CMP), empty microparticles (EMP) and osteogenic medium (OM). $n = 3$, * $p < 0.05$.

mild pipetting (**Fig. 1A**), which indicates that particles were non-aggregating, and therefore favourable for *in vivo* use. An anionic surfactant, Tween 80 was added to the formulations to determine whether particle aggregation would decrease. Contradictingly, faster sedimentation of particles occurred (within 10 min as opposed to over hours for the microparticles without surfactant). Therefore, we can conclude that although exclusion of Tween 80 resulted in larger-sized microparticles, it has better applicability *in vivo*. Moreover, the mean zeta potential and particle size remained unaltered even after 3 months in storage at 4 °C (**Fig. 2A** and **B**). Even after 3 months, particles were easily resuspended by gentle inversion of the storage vial.

The purpose of carrying out the binding study was to establish whether PEDF was encapsulated within the CMPs. Dz13Scr, being anionic in nature, was added to the cationic chitosan, resulting in the formation of an ionic interaction. The particles formed non-aggregating complexes, essentially encapsulating PEDF. In fact, 99.125% of the PEDF was bound with a standard deviation of 0.01%. The bioavailability and the ultimate delivery efficiency of the carrier depends on its cellular uptake profile. **Figure 2C** demonstrates that particles of PEDF encapsulated within chitosan and FITC-Dz13Scr (CMPs) were taken up into cells. Uptake of EMPs was better though not statistically significant ($p = 0.21$).

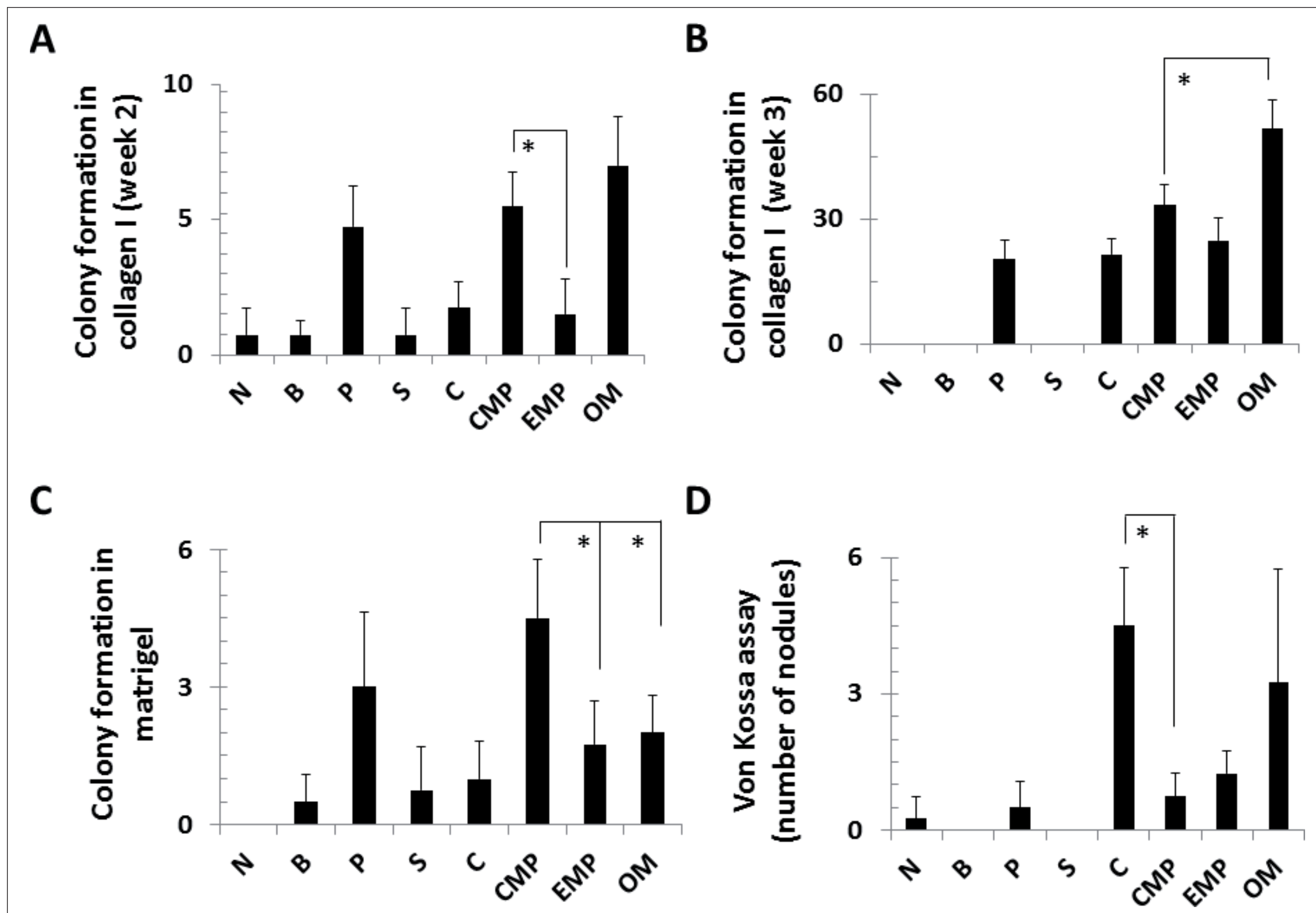


Fig. 3: Pigment epithelium-derived factor (PEDF) microencapsulated within chitosan microparticles (CMP) promotes osteogenic differentiation in monolayer culture. (**A**) Colony formation in collagen I matrix two weeks post-formulation. $n = 3$, * $p < 0.05$. (**B**) Colony formation in collagen I matrix three weeks post formulation. $n = 3$, * $p < 0.05$. (**C**) Colony formation in matrigel. $n = 3$, * $p < 0.05$. (**D**) von Kossa staining of cells as indication of bone mineral nodule formation. $n = 3$, * $p < 0.05$.

### *2.2. Cell-based assays*

The first cell-based study was to rule out gross cytotoxicity of the formulated particles. As shown in **Fig. 2D**, rather promisingly, CMP and EMP demonstrated the highest cell viability in comparison to other positive and negative controls, indicating that both CMP and EMP do not cause harmful effects on MSCs. The difference in the percentage of viable cells between CMP and non-treated control was statistically significant ($p = 0.0001$). CMP and EMP had an equal amount of living cells available and were not statistically significant ($p = 0.42$). In addition, CMP had a far greater percentage of viable cells available when compared to OM but the difference was not statistically significant ($p = 0.07$).

As shown in **Fig. 3A**, OM resulted in the highest number of colonies being formed in collagen I gel, and this is expected as collagen I is the major protein in adult bone. CMP resulted in the second highest number of colonies being formed, a result which was not statistically significant from OM ($p = 0.12$). Conversely, the difference in the number of colonies formed between CMP and EMP was statistically significant ($p = 0.002$). The results were still consistent between weeks 2 and 3, with OM having the highest number of colonies and CMP the second highest ($p = 0.003$) (**Fig. 3B**). At week 3, CMP resulted in a greater number of colonies when compared to PEDF ($p = 0.005$) and chitosan ($p = 0.005$) (**Fig. 3B**). The combined benefit of having PEDF and chitosan (in CMPs) was more apparent at week 3 than week 2.

We further examined the ability of CMPs to form colonies in matrigel, a matrix not closely resembling bone and low in collagen I. Colonies took longer to form - 5 weeks as opposed to 2 weeks in matrigel compared to collagen I respectively. Even in matrigel, CMP formed the highest number of colonies in matrigel (**Fig. 3C**). This was followed by PEDF with the second highest number of colonies, but both were not statistically significant ($p = 0.10$). CMP resulted in a greater number of colonies in comparison to OM (non-significant at $p = 0.01$) and EMP ($p = 0.01$).

Bone mineral formation was quantified by carrying out the von Kossa assay. As shown in **Fig. 3D**, the number of mineral nodules were greater for CMP in comparison to the non-treated control, but this was not statistically significant ($p = 0.10$). In contrast, the difference in the number of mineral nodules formed by chitosan at 0.005% test concentration (chitosan versus CMP) was shown to be statistically significant ($p = 0.003$).

As shown in **Figs. 4A** and **4B**, chitosan induces the highest percentage of mitochondrial abundance. This is followed by starch, the negative control of chitosan, though both are not statistically significant ($p = 0.08$). CMP had a slightly higher percentage of mitochondrial abundance, but it is also not significantly different to non-treated control ($p = 0.09$). Contrary to that, CMP was also not statistically significant with OM ($p = 0.06$).

### *2.3. In vivo bone formation analysis*

Chitosan or PEDF have been known to promote bone regeneration. We therefore carried out an *in vivo* study to determine whether the combination would lead to better bone regeneration. There was no major difference in the average weight of the mice treated with either CMP or EMP (**Fig. 5**). There was also no major difference in the average weight of the mice on the injection and termination day. After the injection of CMP and EMP into the muscle adjacent to the tibia (that is periosteally), each into two groups of twenty mice, and following 8 days, the bone tissues for the left and right hindlimbs of mice were processed for histology and imaged under light microscopy. The bone tissue of the non-injected left hindlimb

Fig. 4: Pigment epithelium-derived factor (PEDF) microencapsulated within chitosan microparticles (CMP) promotes osteogenic differentiation in monolayer culture. (**A**) Colony formation in collagen I matrix two weeks post-formulation. $n = 3$, * $p < 0.05$. (**B**) Colony formation in collagen I matrix three weeks post formulation. $n = 3$, * $p < 0.05$. (**C**) Colony formation in matrigel. $n = 3$, * $p < 0.05$. (**D**) von Kossa staining of cells as indication of bone mineral nodule formation. $n = 3$, * $p < 0.05$.

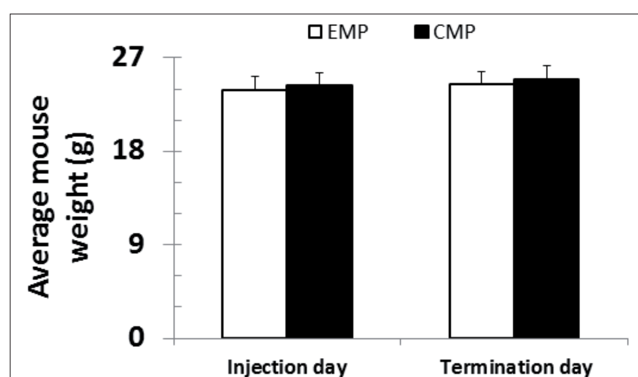


Fig. 5: Average weight of mice. Average weight of mice treated with EMP compared to the average weight of mice treated with CMP on the days of microparticle injection versus study termination. $n = 20$, $p > 0.05$ for all comparisons.

of the mice (that is, the control) (**Figs. 6A** and **6B**) looked different when compared to the right hindlimb of the mice injected with CMP (**Figs. 6C** and **6D**). Osteoid tissue was observed next to the right leg bone tissue (the site which was being treated with CMP periosteally) (**Fig. 6C**). Osteoid tissue observed stood out from the surrounding muscle and bone cortex, and it grew in 'waves' as can be seen by rings budding off from the original cortex. The surrounding cells of the new tissues resembled immune cells, possibly neutrophils, which would be responding to the foreign substance in the body, namely the microparticles. In **Fig. 6D**, adipose tissues and blood vessels were observed near the bone and at the site of injection. There were no behavioural differences between the two cohorts of mice.

In contrast, differences were visible in the bone tissues of the non-injected left leg of the mice treated with EMP (that is, the control) (**Figs. 6E** and **6F**) when compared to the tissues of the injected right leg of the mice treated with EMP. Nonetheless, new tissue, resembling bone was generated as seen in **Fig. 6G**, as it is the site where EMP was injected (right leg of the mice). The result was similar to the result obtained from **Fig. 6C**. However, the formation of new bone in mice being treated with EMP was less efficient in comparison to CMP. In **Fig. 6H**, new bone formation was not visible.

The skeletal muscle tissue of the left leg of mice not treated with either CMP or EMP serve as control groups (**Figs. 7A** and **7C**). In contrast, there were some visible differences in the muscle tissues in the right leg of the mice being treated with either CMP or EMP when compared to the skeletal muscle tissue of the left leg of the mice (**Figs. 7B** and **7D**). The muscle tissue near the injection site of the right leg of the mice being treated with CMP showed growth which did not represent muscle tissue, but was osteoid tissue being formed (**Fig. 7B**). New soft bone tissue was also observed in the

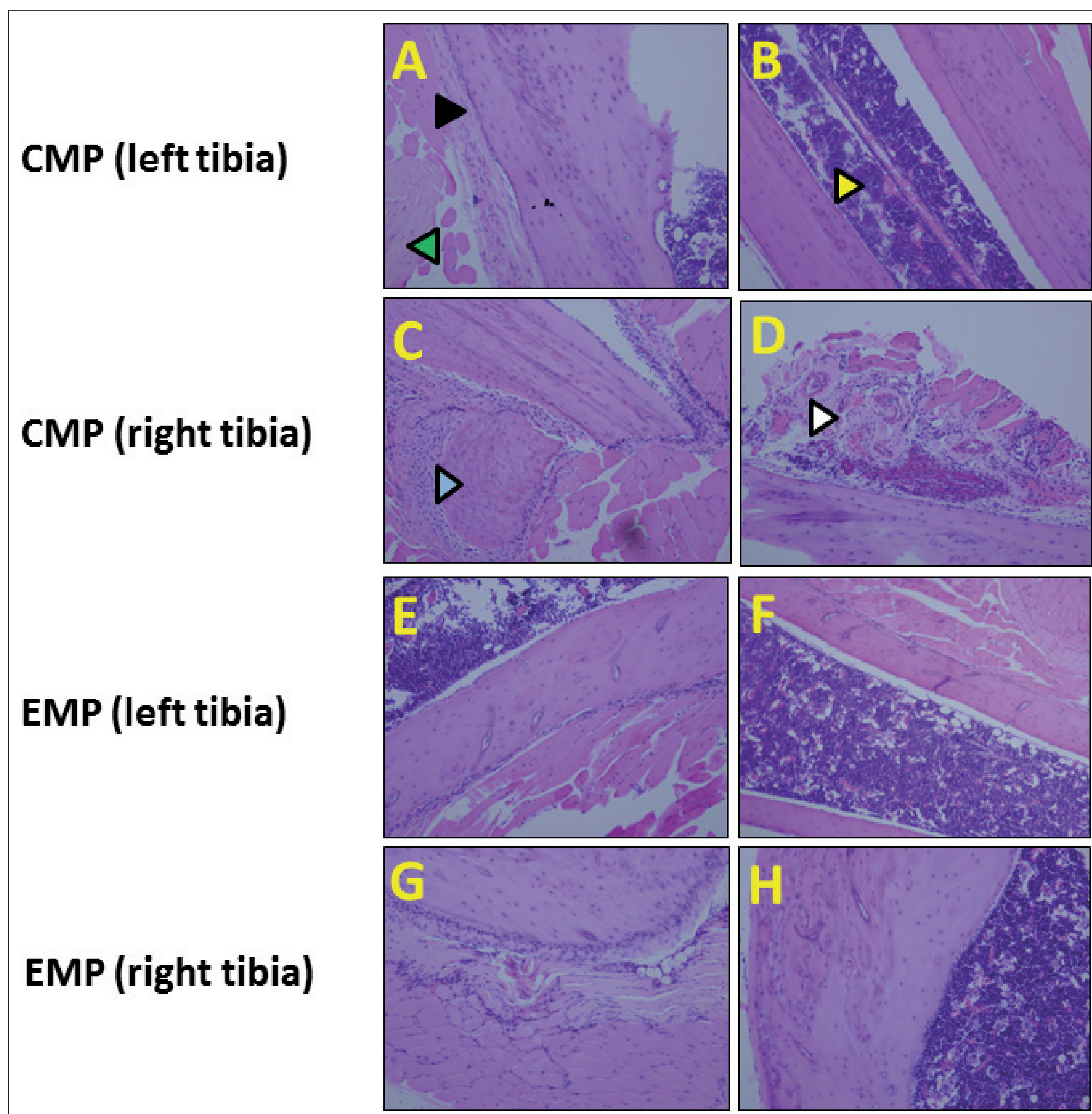


Fig. 6: Pigment epithelium-derived factor (PEDF) microencapsulated within chitosan microparticles (CMP) induces bone regeneration. (**A,B**). Left bone of the mice treated with CMP. (**C,D**). Right bone of the mice treated with EMP. (**E,F**). Left bone of the mice treated with EMP. (**G,H**). Right bone of the mice treated with EMP. *Arrowheads*: *black*, bone cortex, *yellow*, bone marrow, *white*, inflammatory cells, *green*, muscle tissue, *blue*, newly formed bone tissue.

right skeletal muscle tissue near the injection site of the right leg being treated with EMP (**Fig. 7D**).

For the pancreas, there was a visible difference in the size of the islet of Langerhans. **Figure 8A** shows normal pancreatic tissue in the CMP group of mice, but when the mice were treated with EMP for a week, the pancreatic tissue had smaller islets of Langerhans (**Fig. 8B**). Furthermore, there was a difference in the colour of the secretory acini as it was more pink (that is, had more acidophilic regions) with EMP in comparison to the mice being injected with CMP which was more purple in colour (had more basophilic regions). Another difference between the two groups was that the mice being injected with CMPs resulted in several large, circular and completely clear vacuoles (**Fig. 8C**). On the other hand, the mice treated with EMPs resulted with many tiny, circular white vacuoles scattered throughout (**Fig. 8D**). This is not commonly seen in normal pancreatic tissues.

## 3. Discussion

Chitosan has the potential for cell adhesion and proliferation as well as supporting the survival of MSCs (Tan et al. 2014). PEDF, a protein that promotes osteogenesis, has the capability to differentiate MSCs into osteoblasts (Gattu et al. 2013). Both biologicals could be useful therapeutic agents against bone defects such as fractures and osteoporosis. In this study, we seminally demonstrated that the combination of chitosan microparticles encapsulating PEDF can enhance the formation of bone and support the viability of MSCs in culture.

CMP and EMP had the highest MSC viability, thus illustrating their lack of cytotoxicity. Chitosan has the potential to trigger osteogenic differentiation in MSCs, plus increase the viability of osteoblasts and reduce the number of osteoclasts. It is also pro-apoptotic in osteosarcoma cells, but not in osteoblasts. Furthermore, it has the potential to reduce the viability of human breast and prostate cancer cells (Tan et

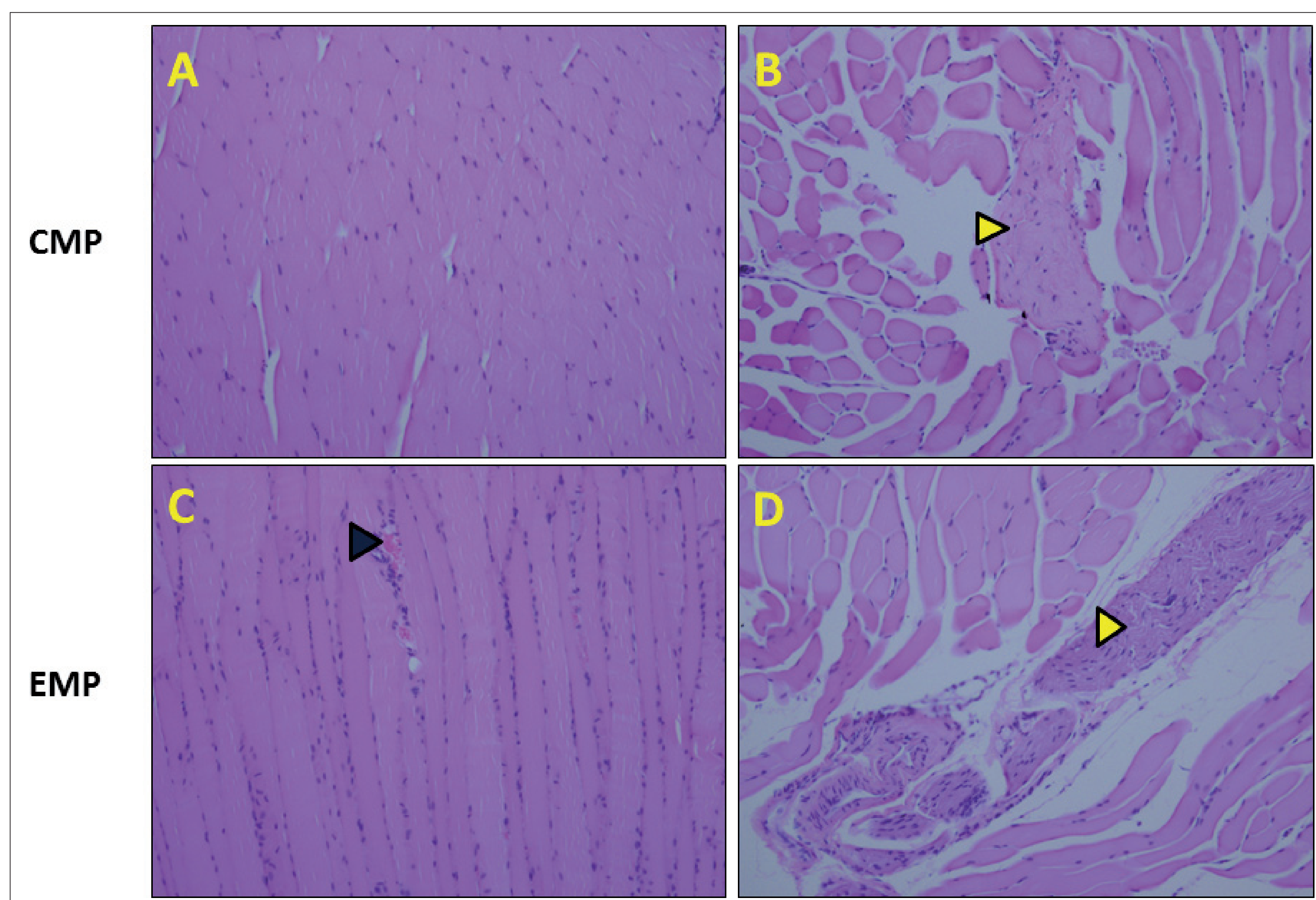


Fig. 7: Pigment epithelium-derived factor (PEDF) microencapsulated within chitosan microparticles (CMP) induces soft bone tissue adjacent to skeletal muscle tissues. (**A**). Skeletal muscle tissue of the non-injected left leg of mice treated with CMP. (**B**). Skeletal muscle tissue of the injected right leg of mice treated with CMP. (**C**). Skeletal muscle tissue of the non-injected left leg of mice treated with EMP. (**D**). Skeletal muscle tissue of the injected right leg of mice treated with EMP. *Arrowheads*: *black*, red blood cells, *yellow*, formation of osteoid tissue.

al. 2014). Hence, chitosan is a promising agent for management of bone trauma, bone healing and bone tumours.

Collagen I is known to be one of the most abundant proteins in the human body and one that supports and strengthens the bone (Fallas et al. 2010). It is involved in bone healing, maturing as well as aging. In this study, CMP was found to have the ability to form the most number of colonies in collagen I. Chitosan can increase osteopontin (a glycoprotein that facilitates bone regeneration) as well as collagen I expression (Tan et al. 2014). PEDF is avidly bound to collagen I, which indicates that collagen I plays an important role in the function of PEDF (Ek et al. 2007a). CMP obtained the highest number of colonies formed in collagen I matrix, demonstrating the potential of the combination of chitosan microparticles and PEDF for *in vivo* bone regeneration.

Bone regeneration is mediated via MSCs and osteoprogenitor cells (Jones and Yang 2011). CMPs were seen to induce a reasonably low number of mineralised (calcium-containing) nodules compared to free chitosan, but more than the control. Thus, CMP possesses the ability to induce differentiation of osteoprogenitor cells and facilitate bone formation. As a side-note, free chitosan has a far greater potential to form bone mineral nodules relative to CMP which is concordant with our previous studies (Tan et al. 2014; Shao et al. 2014).

Mitochondria are important organelles that have essential roles in ATP production, oxidative phosphorylation and various other signalling events (Lin et al. 2015). Many clinical diseases occur due to mitochondrial dysfunction and therefore, the number and health of mitochondria is crucial in order for the cells to function, and this is also the case for MSCs (Lin et al. 2015). CMPs or EMPs did not perturb the abundance of mitochondria, once again demonstrating their lack of cytotoxicity.

*In vivo*, both CMP and EMP resulted in bone regeneration. However, bone regeneration was found to occur within a shorter period of time in CMP than EMP. Several studies have demonstrated that the stimulation of angiogenesis in bone, when induced by vascular endothelial growth factor (VEGF), can promote repair mechanisms during bone injury (Takenaka et al. 2005; Tombran-Tink et al. 2004). However, the addition of PEDF, an angiogenesis inhibitor, to chitosan microparticles could possibly detract from proper bone regeneration. This was ruled out in our study, as *in vivo*, both CMP and EMP resulted in bone regeneration. The presence of a foreign object (microparticles), or perhaps even the new osteoid tissue being formed, stimulated the body to produce an immune response by increasing the influx of inflammatory cells to the site of injection (Anderson et al. 2008). It is noteworthy that the acute inflammation at the tissue injection site did not alter mouse use of the hindlimbs or overall behaviour. Further studies looking at long-term effects of CMP injection and effects due to repeat dosing are warranted.

Other than that, the islets of Langerhans in mice treated with EMP were smaller than normal, whilst there was no difference in the CMP-treated cohort. Islet of Langerhans consist of glucagon-releasing alpha cells, insulin-releasing beta cells and somatostatin-producing delta cells (Nadal et al. 1999). PEDF is known to have an effect on insulin: the short term use of PEDF can cause a reduction in insulin signal transduction and this can lead to the stimulation of lipolysis of adipose tissues as well as a reduction in insulin sensitivity if it is used long-term (Carnagarin et al. 2015). Additionally, differences were seen in the pancreatic tissues of the mice treated with EMP: decreased density of the basal basophilic zones of the secretory acini, which resulted in the unusually high representation with pink hue when pancreases were

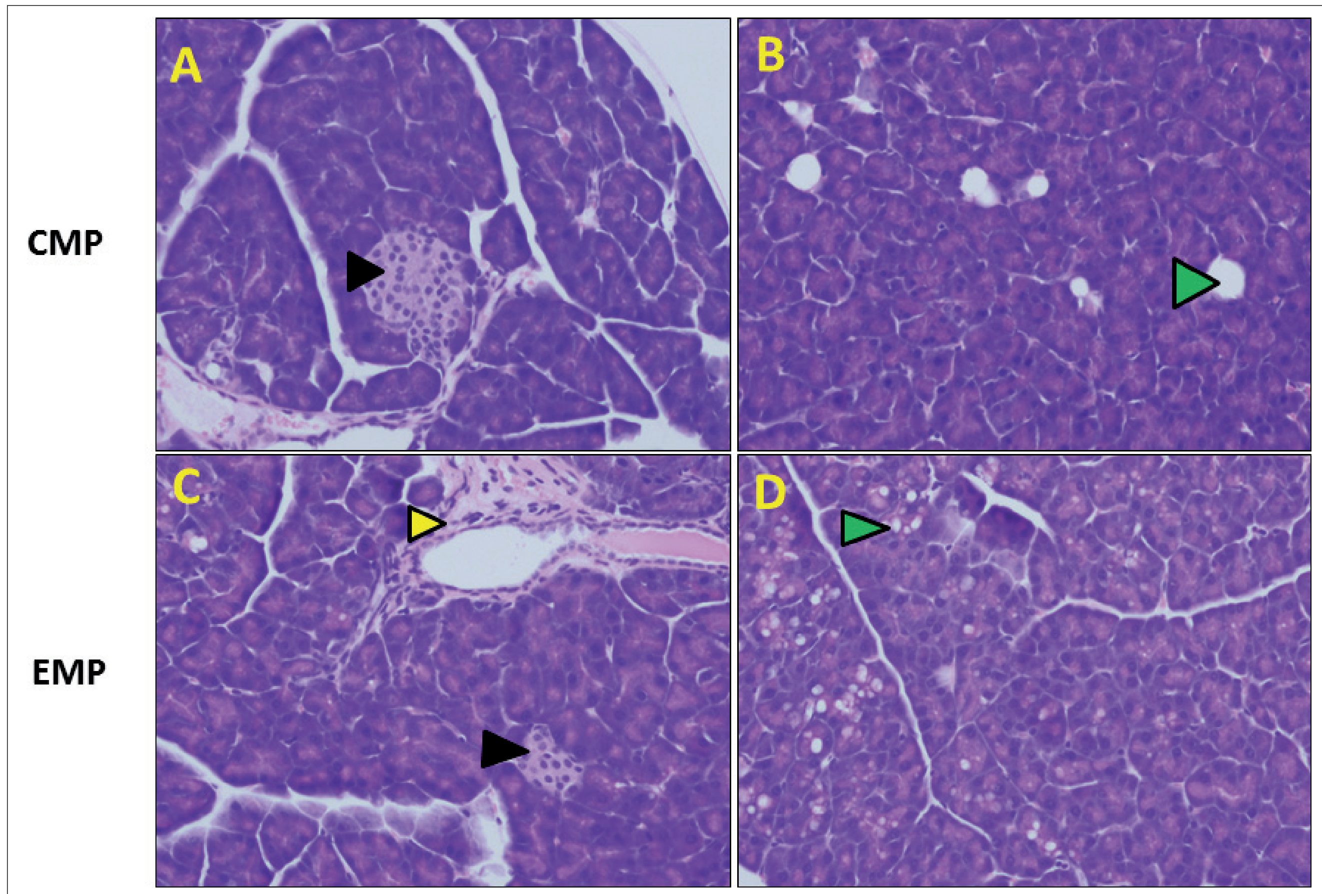


Fig. 8: Pigment epithelium-derived factor (PEDF) microencapsulated within chitosan microparticles (CMP) causes changes to pancreatic tissues. (**A,B**). Pancreatic tissue of mice treated with CMP. (**C,D**). Pancreatic tissues of mice treated with EMP. *Arrowheads*: *black*, islets of Langerhans, *yellow*, interlobular duct, *green*, vacuoles.

stained with H&E. This was consistent with our previous study with free chitosan (Tan et al. 2014). The promising finding was that this phenomenon was not noted in the CMP group, indicating that PEDF was able to neutralise this perturbing effect of the EMP, though the mechanisms underlying this are unknown.

Thus, summarily our studies show that PEDF microencapsulated within chitosan was able to maintain its efficacy for regeneration of bone. The long-term safety of this technology needs to be evaluated, as well as the efficacy gauged in clinical models of disease such as osteoporosis and bone fractures.

In summary, PEDF microencapsulated within chitosan can induce osteogenic differentiation in MSCs and increase osteoblast viability *in vitro* as well as enhance bone regeneration *in vivo*. Collectively, these findings demonstrated that the combination appears to be safe to the surrounding tissues and is promising for bone regeneration. Further studies are required to be performed in bone defect models to evaluate the combination's use for bone tissue regeneration in the future.

## 4. Experimental

### 4.1. CMP formulation

Chitosan and Dz13Scrambled (Dz13Scr, an oligonucleotide) were obtained from Sigma-Aldrich (St. Loius, MO, USA). The particles were formulated using a vortex-assisted complex coacervation method (Tan et al. 2014; Dass et al. 2007). Polycationic chitosan at 0.005% (in 25 mM sodium acetate (SA) buffer) and 100 nM of PEDF (Bioproducts MD, Bethesda, MD, USA) were added to an equal volume (75 µL) of 10 µg of polyanionic Dz13Scr (Zhang et al. 2004) (in 50 mM sodium sulfate buffer) and vortexed at high speed for 5 s at room temperature. The polyanionic Dz13Scr was then added to the polycationic chitosan and further vortexing for 30 s was performed in order to microencapsulate PEDF.

### 4.2. Particle sizing and zeta potential

Microparticles were tested (in triplicate) for hydrodynamic diameter and surface charge – on the day of formulation and again following 3 months storage at 4 °C after formulation. A surfactant, Tween 80 (Sigma) was also added to determine whether it prevents agglomeration of particles by acting as a dispersant. The particle size and zeta potential were measured on a Zetasizer Nano ZSP (Malvern, UK).

### 4.3. Binding

After formulation, three independent CMP suspensions were centrifuged at 1000 *g* for 2 min. The supernatants containing the unbound PEDF were removed and analysed using the enzyme-linked immunosorbent assay (ELISA) for PEDF (Millipore, Darmstadt, Germany), and the amount of PEDF bound to CMPs was determined.

### 4.4. Cellular uptake

CMPs and EMPs were incubated with mesenchymal stem cells (MSCs) for 24 h, then cells were fixed with 4% paraformaldehyde and nuclei counterstained with 4′,6′-diamino-2-phenylindole, DAPI (Sigma) as performed previously (Dass et al. 2002). MSCs were isolated from the marrow resident in the long bones of 6 week-old Balb/c mice, and were kept under liquid nitrogen storage and thawed as required. Cells were cultured according to current standard procedures and conditions in humidified 5% $CO_2$ at 37 °C and expanded in complete medium. Cells were seeded in 96-well plates, and when they reached 60-80% confluency 24 h later, treatments were added. For the uptake study, the Dz13Scr oligonucleotide was labelled with fluorescein isothiocyanate (FITC) to enable fluorometric tracking of particles into and within cells. An inverted Olympus IX51 (Olympus, Melbourne, Australia) fluorescence microscope was used for imaging.

### 4.5. Cell viability assay

The positive control for this assay included the osteogenic medium (OM) and the negative controls comprised of the non-treated control (N), bovine serum albumin (BSA), starch (S) as well as the empty chitosan microparticles (EMP) without the PEDF being encapsulated. Unencapsulated (free) PEDF (P) and chitosan (C) controls were also included. These controls were used for each of the biological assays performed. MSCs were plated in 96-well plates and treated at 50% confluency for 24 h. The CT-Blue reagent (Promega, Sydney, Australia) was added into each well and incubated at 37 °C for 1 h, and extent of resazurin to resorufin conversion read fluorometrically at excitation of 560 nm and emission of 610 nm in an Enspire 2300 multimode microplater reader (Waltham, Massachusetts, USA). The assay was done in triplicates and repeated.

### 4.6. *Mitochondrial abundance*

MSCs were treated for 24 h with particles and controls, then labelled with 100 nM MitoTracker Red FM (a carbocyanine-based red-fluorescent mitochondrial stain) (Invitrogen, Scoresby, Australia) for 30 mins at 37 °C. Excess probe was then washed off by rinsing four times with PBS prior to visualisation in a 96-well plate under the TRITC channel on a fluorescence microscope after mounting with glycerol (100%). Image J imaging software (NIH, MD, USA) was utilised to analyse mitochondrial abundance based on the corrected total cell fluorescence (CTCF) of each well of the conditions tested. The assay was done in triplicates and repeated.

### 4.7. *Collagen I colony formation*

Serum-free media was used to wash the exponentially-growing MSCs after being harvested. The final concentration of the collagen gel (BD Biosciences, Bedford, MA) was 1.5 mg/ml in complete medium, consisting of 10% DMEM and 1% FCS (Dass et al. 2006). The bottom layer of the gel was poured and solidified in a 96-well plate (Ek et al. 2007a). The top layer containing 1000 MSCs in suspension per well was poured and solidified. Plates were then placed in a 37°C/5% $CO_2$ incubator for 21 days to allow growth, then colonies were counted. Wells were topped up with serum-free medium to prevent dehydration of the gels. A colony was defined as a cluster of more than three viable-looking cells. The assay was done in triplicates and repeated.

### 4.8. *Matrigel colony formation assay*

For this assay, 96-well plates were coated with a 1:2 dilution of matrigel (BD Biosciences) and the wells were filled with complete growth medium (Dass et al. 2006). Cells were seeded in serum-free medium at a density of 1000 per well, and were incubated for 5 weeks at 37 °C. Wells were topped up with complete growth medium to prevent dehydration of the gels. A colony was defined as a cluster of more than three viable-looking cells. The assay was done in triplicates and repeated.

### 4.9. *Mineral nodule formation*

MSCs in monolayer culture were treated with CMPs at different timepoints (7, 14 and 21 days) and mineral formation monitored *via* von Kossa staining. Cells were fixed with 4% paraformaldehyde for 30 min (Ek et al. 2007b). Mineralised nodules were visualised by staining the plates with 5% silver nitrate (Sigma) and placing under light for 30 min. Plates were treated with 5% sodium thiosulphate (Sigma) prior to rinsing with water before the images were acquired on the inverted Olympus IX51 microscope.

### 4.10. *In vivo studies*

Ethics approval (AEC 2014/37) was obtained from the Curtin University Animal Ethics Committee on the 20th of October 2014. Forty 12-week old male Balb/c mice were sourced from the Animal Resources Centre (Perth, Australia), and anaesthetised with isoflurane. Twenty mice were injected with 50 µl of CMP containing PEDF and the other twenty mice were injected with 50 µl of EMP into their right hindlimbs, periosteally (next to the tibia). The mice were then carefully placed on to a heat pad awaiting full recovery from anaesthesia. These implants were left for 8 days to observe the early onset of *de novo* osteogenesis *in vivo*. Mice were then euthanised, and limbs plus pancreas harvested. Tissues were processed and sectioned at 4 µm and stained with haematoxylin and eosin (H & E) before the images were acquired. Sections were imaged using an Olympus CX31 (Olympus, Melbourne, Australia) upright microscope.

### 4.11. *Statistical analysis*

*In vivo* and *in vitro* data were analysed for statistical significance with the *t*-test. Mean ± standard deviation are presented in graphs, and a probability ($p$) value of $< 0.05$ was used to indicate significance for all the assays.

Conflict of interest: There is no conflict of interest in performing the studies mentioned, as well as in the preparation and submission of this manuscript.

Acknowledgement: The authors acknowledge a Curtin University Academic50 grant support to CRD.

## References


Anderson JM, Rodriguez A, Chang DT (2008) Foreign body reaction to biomaterials. Semin Immunol 20: 86 - 100.

Broadhead ML, Akiyama T, Choong PF, Dass CR (2010) The pathophysiological role of PEDF in bone diseases. Curr Mol Med 10: 296 - 301.

Broadhead ML, Dass CR, Choong PF (2009) Cancer cell apoptotic pathways mediated by PEDF: prospects for therapy. Tr Mol Med 15: 461 - 7.

Carnagarin R Dharmarajan AM, Dass CR (2015) PEDF-induced alteration of metabolism leading to insulin resistance. Mol Cell Endocrinol 401: 98 - 104.

Cheng XM, Li Y, Zuo Y, Zhang L, Li J, Wang H (2009) Properties and in vitro biological evaluation of nanohydroxyapatite/ chitosan membranes for bone guided regeneration. Mater Sci Eng: C 29: 29 - 35.

Dash M, Chiellini F, Ottenbrite RM, Chiellini E (2011) Chitosan – a versatile semi-synthetic polymer in biomedical applications. Prog Polym Sci 36: 981 - 1014.

Dass CR, Contreras KG, Dunstan DE, Choong PF (2007) Chitosan microparticles encapsulating PEDF plasmid demonstrate efficacy in an orthotopic metastatic model of osteosarcoma. Biomaterials 28: 3026 - 33.

Dass CR, Ek ET, Contreras KG, Choong PF (2006) A novel orthotopic murine model provides insights into cellular and molecular characteristics contributing to human osteosarcoma. Clin Exp Metastasis 23: 367 - 80.

Dass CR, Saravolac EG, Li Y, Sun LQ (2002) Cellular uptake, distribution and stability of 10-23 deoxyribozymes. Antisense Nucl Acid Drug Dev 12: 289 - 99.

Ek ET, Dass CR, Contreras KG, Choong PF (2007a) Inhibition of orthotopic osteosarcoma growth and metastasis by multitargeted antitumor activities of pigment epithelium-derived factor. Clin Exp Mets 24: 93 - 106.

Ek ET, Dass CR, Contreras KG, Choong PF (2007b) PEDF peptides inhibit osteosarcoma growth and metastasis in mice. J Orthop Res 25: 1671 - 80.

Fallas JA, O'Leary LE, Hartgerink JD (2010) Synthetic collagen mimics: self-assembly of homotrimers, heterotrimers and higher order structures. Chem Soc Rev 39: 3510 - 27.

Gattu AK, Swenson ES, Iwakiri Y, Samuel VT, Troiano N, Berry R, Church CD, Rodeheffer MS, Carpenter TO, Chung C (2013) Determination of mesenchymal stem cell fate by pigment epithelium-derived factor (PEDF) results in increased adiposity and reduced bone mineral content. FASEB J 27: 4384 - 94.

Jiang T, James R, Kumbar S, Laurencin CT (2014) Chitosan as a biomaterial: structural, properties, and applications in tissue engineering and drug delivery. Nat Synth Biomed Polym 5: 91 - 113.

Jones E, Yang X (2011) Mesenchymal stem cells and bone regeneration: Current status. Injury 42: 562 - 568.

Li F, hyte N, Niyibizi C (2012) Differentiating multipotent mesenchymal stromal cells generate factors that exert paracrine activities on exogenous MSCs: Implications for paracrine activities in bone regeneration. Biochem Biophys Res Commun 426: 475 - 479.

Lin H, Liou CW, Chen SD, Hsu TY, Chuang JH, Wang PW, Huang ST, Tiao MM, Chen JB, **Lin** TK, Chuang YC (2015) Mitochondrial transfer from Wharton's jelly-derived mesenchymal stem cells to mitochondria-defective cells recaptures impaired mitochondrial function. Mitochondrion 22; 31 - 44.

Nadal A, Quesada I, Soria B (1999) Homologous and heterologous asynchronicity between identified α-, β- and δ-cells within intact islets of Langerhans in the mouse. J Physiol 517: 85 - 93.

Papadimitropoulos A, Scotti C, Bourgine P, Scherberich A, Martin I (2015) Engineered decellularized matrices to instruct bone regeneration processes. Bone 70: 66 - 72.

Petite H, Viateau V, Bensaïd W, Meunier A, de Pollak C, Bourguignon M, Oudina K, Sedel L, Guillemin G (2000) Tissue-engineered bone regeneration. Nature Biotechnol 18: 959 - 63.

Serra IR, Fradique R, Vallejo MC, Correia TR, Miguel SP, Correia IJ (2015) Production and characterization of chitosan/gelatin/β-TCP scaffolds for improved bone tissue regeneration. Mater Sci Eng: C 55: 592 - 604.

Shao P, Wei Y, Dass CR, Zhang G, Wu Z (2014) Systemic delivery of free chitosan accelerates femur fracture healing in rats. Curr Drug Targets PMID: 25300779.

Shrivats AR, Alvarez P, Schutte L, Hollinger JO (2014) Bone regeneration. In: Lanza R, Langer R, Vacanti JP (eds.) Principles of Tissue Engineering, 4th ed., pp. 1201 - 21.

Takenaka K, Yamagishi S, Jinnouchi Y, Nakamura K, Matsui T, Imaizumi T (2005) Pigment epithelium-derived factor (PEDF)-induced apoptosis and inhibition of vascular endothelial growth factor (VEGF) expression in MG63 human osteosarcoma cells. Life Sci 77: 3231 - 3241.

Tan ML, Choong PF, Dass CR (2009) Cancer, chitosan nanoparticles and catalytic nucleic acids. J Pharm Pharmacol 61: 3 - 12.

Tan ML, Shao P, Friedhuber AM, van Moorst M, Elahy M, Indumathy S, Dunstan DE, Wei Y, Dass CR (2014) The potential role of free chitosan in bone trauma and bone cancer management. Biomaterials 35: 7828 - 38.

Tombran-Tink J, Barnstable CJ (2004) Osteoblasts and osteoclasts express PEDF, VEGF-A isoforms, and VEGF receptors: possible mediators of angiogenesis and matrix remodeling in the bone. Biochem Biophys Res Commun 316: 573 - 579.

Vimalraj S, Selvamurugun N (2014) MicroRNAs expression and their regulatory networks during mesenchymal stem cells differentiation toward osteoblasts. Int J Biol Macromol 66: 194 - 202.

Zhang G, Dass CR, Sumithran E, Di Girolamo N, Sun LQ, Khachigian LM (2004) Effect of deoxyribozymes targeting c-jun on tumor growth and angiogenesis in mice. J Natl Cancer Inst 96: 683 - 96.